Material and structural response of Textile Reinforced Concrete with fibres

Respuesta estructural y material del Hormigón Reforzado con Textiles considerando la adición de fibras

Julie Devènes[a], Gonzalo S.D Ulzurrun[b], Álvaro Picazo[c], Leonardo Todisco[d], Carlos Zanuy[e] Alejandro Enfedaque[f], Miguel Fernández Ruiz[g]

Universidad Politécnica de Madrid: [a] j.devenes@upm.es, [b] g.ulzurrun@upm.es, [c] a.picazo@upm.es, [d] leonardo.todisco@upm.es, [e] carlos.zanuy@upm.es, [f] alejandro.enfedaque@upm.es, [g] miguel.fernandezruiz@upm.es

ABSTRACT

This paper explores the tensile response of Textile Reinforced Concrete (TRC) incorporating polyolefin fibres from a material and structural perspective. The material response is characterized for the micro-concrete and carbon textile used, and detailed analyses are presented on the influence of the fibres. A series of tensile tests on TRC ties analyse the composite action of TRC and show that the orientation of the textile significantly influences its performance. According to the experimental results, the failure mode depends on the orientation and undulations of the textile, which can lead to delamination failures. A theoretical model predicts the tensile behaviour of TRC, including cases with and without delamination.

RESUMEN

Este artículo explora la respuesta en tracción desde una perspectiva material y estructural del Hormigón Reforzado con Textiles (HRT) incorporando fibras de poliolefina. Se caracteriza la respuesta del micro-hormigón y del textil de carbono utilizados, y se presentan análisis detallados sobre la influencia de las fibras. Se presenta una serie de ensayos de tracción en tirantes de HRT analizando la acción compuesta del HRT y muestran que la orientación del textil influye significativamente en su comportamiento. Según los resultados experimentales, el modo de fallo depende de la orientación y de las ondulaciones del textil, que pueden conducir a fallos por delaminación. Se indica un método analítico para reproducir el comportamiento observado a tracción del HRT, incluyendo casos con y sin delaminación.

KEYWORDS: textile reinforced concrete, structural response, experimental programme
PALABRAS CLAVE: hormigón reforzado con textil, respuesta estructural, programa experimental

1. Introduction

The environmental footprint of concrete is a matter of concern [1],[2] and is pushing the scientific and practitioner communities to actively look for more rational manners to use it. This comprises efforts both on the material and structural performance. From a material perspective, the high carbon footprint of cement production is primarily due to the production of clinker. Reducing clinker content by substituting alternative materials, such as calcined clays, while optimizing mix designs, has proven to be an effective way to lower emissions [3], [4], although it raises questions on the durability and protection against corrosion. On the structural side, minimizing material usage is the strategy to be followed, by designing more efficient new structures (as well as assessing the latent resistance reserves of existing ones).

In this context, Textile Reinforced Concrete (TRC) emerges as a more sustainable alternative to conventional reinforced concrete [5]. TRC incorporates a bidirectional textile fabric, typically composed of carbon or alkali-resistant glass (replacing metallic reinforcement) embedded within a cementitious matrix. Unlike traditional steel rebars, the non-corrosive textiles eliminate any need for passivation, which allows for using low-clinker cements. In addition, as no concrete cover is required for the reinforcement (other than static needs), thinner and lighter structures can be built.

Concerning the textiles, innovations such as coated and impregnated rovings have enhanced the bond strength between fabric and matrix, improving stress distribution and durability [6], [7]. However, the brittle nature of TRC under tension remains a key challenge, as it limits redistribution of internal forces and overall structural performance [8].

In order to make a step forward in this topic, the present study investigates two complementary strategies to enhance the structural behaviour of TRC by increasing its toughness. At the material level, polyolefin fibres are incorporated into the cementitious matrix to improve toughness and control cracking. At the structural level, a "fuse strategy" is explored by intentionally designing weak zones governed by the pull-out behaviour of the fabric, enhancing deformation capacity and avoiding brittle failure modes.

An extensive experimental program was conducted to select and characterize the components: the polyolefin fibre-reinforced matrix, the carbon-textile fabric, and their combined tensile behaviour as TRC. The experimental results are analysed with respect to physical parameters, including fibre dosage, fibre orientation, and fabric undulation. Additionally, the research proposes a simplified analytical model capable of predicting the tensile response of TRC, accounting for delamination cracks phenomena.

2. Material selection and characterization

2.1 Characterization of the micro-concrete matrix integrating polyolefin fibres

Two micro-concrete premixes were considered, combined with different ratios of polyolefin synthetic macro-fibres at dosages of 0 kg/m^3, 4.5 kg/m^3 (V_f = 0.5 %) and 10 kg/m^3 (V_f = 1.1 %). The length of the fibres is selected in order to enable an efficient structural role. The two micro-concrete mixes M1 and M2 are presented in Table 1 as well as the polyolefin fibres properties in Table 2.

Table 1. Composition of micro-concrete M1 and M2

	M1	M2
Binder (CEM III/AS-42,5)	18%	27%
Water added to premix	14%	11%
Maximum aggregate size	2 mm	4 mm

Table 2. Properties of polyolefin fibres

Length	48 mm
Density	0.91 g/cm^3
Equivalent diameter	0.84
Tensile strength	465-530 MPa
Young modulus	8.8 GPa

To ensure the flow of the fibres through the carbon-textile fabric and to facilitate the casting of thin elements, the matrix required to be sufficiently fluid with aggregates of small size, while keeping at the same time a uniform distribution of fibres. Slump tests with mini-Abrams cone [9] were performed to characterise the self-compacting matrix. On the other hand, compressive tests on cube specimens 40x40x40 mm^3 [10] and three-points bending tests on specimens 40x40x160 mm^3 [11] were conducted to characterize the mechanical properties at the hardened state.

The slump tests showed good performance of the two micro-concrete types with sufficient fluidity, Figure 1 (c). The addition of fibres had very few impacts on the slump behaviour. Nevertheless, the distribution of fibres in the matrix significantly depended on amount of water added to the premixes. For higher amounts of water (17% and 12% for micro-concrete M1 and M2 respectively), the dispersion of fibres was not homogenous (the fibres were not entrained during the casting process which led to accumulation of fibres). Therefore, the amount of water added was reduced to 14% and 11% for micro-concrete M1 and M2 respectively (see Table 1), to find an optimal combination of fluidity and fibres homogeneous distribution.

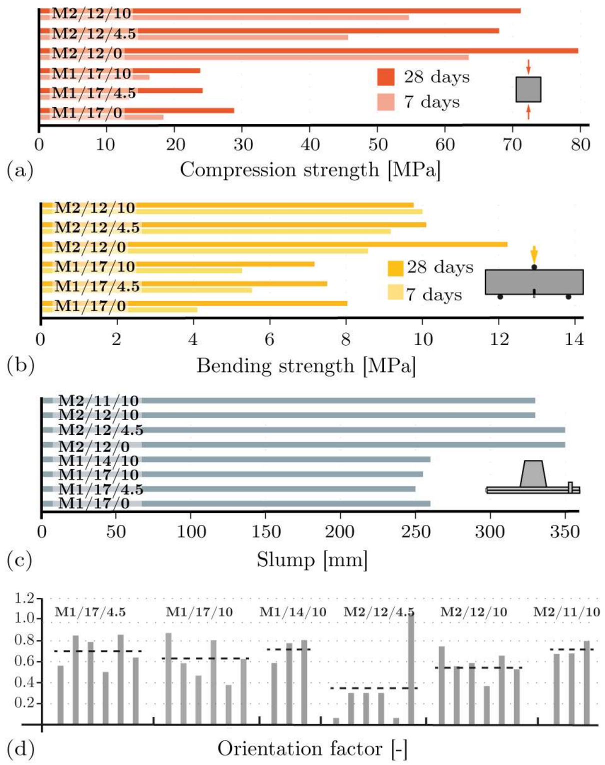

Figure 1. Characterization of micro-concrete premixes M1 and M2

Both micro-concrete M1 and M2 exhibited good mechanical performances, showing high flexural (Figure 1 (b)) and compressive strength (Figure 1 (a)). The micro-concrete M1 had standard performance, while the micro-concrete M2 had high performance. The fibres present on the micro-concrete had a significant role in the toughness of the specimens. During the bending tests, the specimens without fibres broke suddenly, with plain fracture surface. In contrast, the specimens with fibres exhibited a higher deformation capacity, with crack opening and irregular fracture surfaces. On the fracture sections of the bending specimens, the fibres were counted to estimate the fibre orientation factor (θ). This is the relation between the number of fibres in the fracture section and the theoretical number of fibres. The orientation factors for each bending specimens tested for micro-concrete M1 and M2 are shown on Figure 1 (d).

Following the experimental results, micro-concrete M1 was kept for the rest of the investigation. This is justified by the lower cement content (and associated environmental impact) while having reasonable mechanical performance. Additional material tests performed for micro-concrete M1 are presented in [12].

2.2 Characterization of the carbon-textile fabric

Concerning the reinforcement, a bi-directional carbon-textile fabric with a sand-coated surface was used, shown in Figure 2.

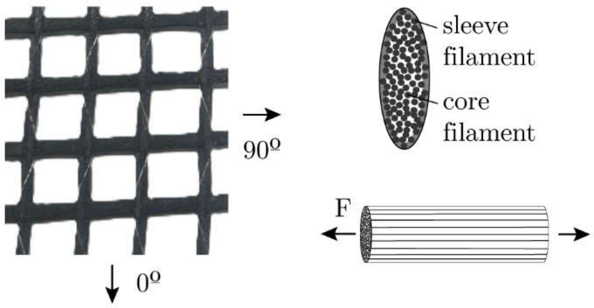

Figure 2. carbon-textile bi-directional fabric

Table 3. Properties of carbon-textile fabric according to manufacturer [13]

Direction α_r		0º	90º
Linear density λ_r	[tex/roving]	2x1600	3200
Net cross section A_r	[mm²/m]	105	105
	[mm²/roving]	1.79	1.79
Grid spacing e_r	[mm]	17	17
Elastic modulus E_r	[GPa]	240	40
Nominal perimeter U_r	[mm]	11	12

Tensile tests were conducted on single roving's extracted from the fabric, with different specimen configurations illustrated in Figure 3.

Specimen (a): This configuration consists of a single roving clamped at both ends. Failures frequently occurred in or near the clamping zone (failure type 1), even when timber plates were used as protective layers to minimize stress concentrations. The results of such setup were thus disregarded as they are not representative of the material response.

Specimens (b-c): To reduce clamping-related failures, it was explored to embed the roving in concrete at both ends. Specimen (b) consists of one single roving, while Specimen (c) includes five rovings. For Specimen (b), failure occurred also at the interface between the concrete and the roving, likely due to stress concentrations or interface damage caused during demoulding. Specimen (c) exhibited failures either at the interface (failure type 2) or along the free length (failure type 3). However, uniform activation of all rovings was not possible. Consequently, these test setups were also disregarded as they were not providing reliable values of the material response

Specimens (d-e): These configurations are designed to distribute forces more smoothly into the rovings. The clamping areas are reinforced with five additional rovings, and the specimen shape is optimized for gradual load introduction. The material used at both ends is an epoxy resin [14]. Specimen (d) has a long free length (320 mm), while Specimen (e) has a short free length (35mm) to simulate conditions like those in a concrete specimen with a crack. To avoid damage of the specimens, timber bars are glued to the resin extremities to avoid any unvoluntary damage during placing of the specimens. For these configurations, failures occurred systematically in the free length of the rovings, with low scatter and similar results independently of the free length selected.

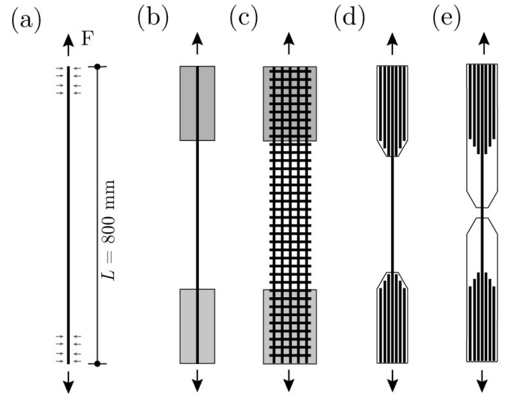

Figure 3. carbon-textile specimens typology

The results obtained for each specimen configuration are summarized in Table 4. Specimens (d) and (e) provide a reliable estimate of the tensile strength of the rovings, comparable to the values obtained with the Castan grips method [7]. Additionally, these configurations ensure failure occurs in the free length of the specimens, avoiding stress concentrations in the clamping or embedded zones.

Table 4. Results of tensile tests on carbon-textile rovings for different specimens typology (a) to (e) (values in brackets refer to number of tests and standard deciation respectively).

Type	Orientation [º]	Tensile Strength [MPa]	Failure type
(a)	90	1184 (5, 191)	1
(a)	0	918 (5, 75)	1
(b)*	90	1373 (4, 100)	2
(b)*	0	1398 (4, 132)	2
(c)*	90	1496 (5, 76.5)	2, 3
(d)	0	1665 (3,145)	3
(e)	0	1668 (2, 102)	3

*Initial damage of the roving cannot be excluded

The failure of the carbon-textile is characterized by a sudden rupture. This behaviour is further illustrated in Figure 4, which highlights the abrupt failure of the roving in specimen (e) as recorded by a high-speed camera (FASTCAM NOVA S9 de Photron) at a frame rate of 4000 frames per second with a shutter speed of 1/12000 seconds.

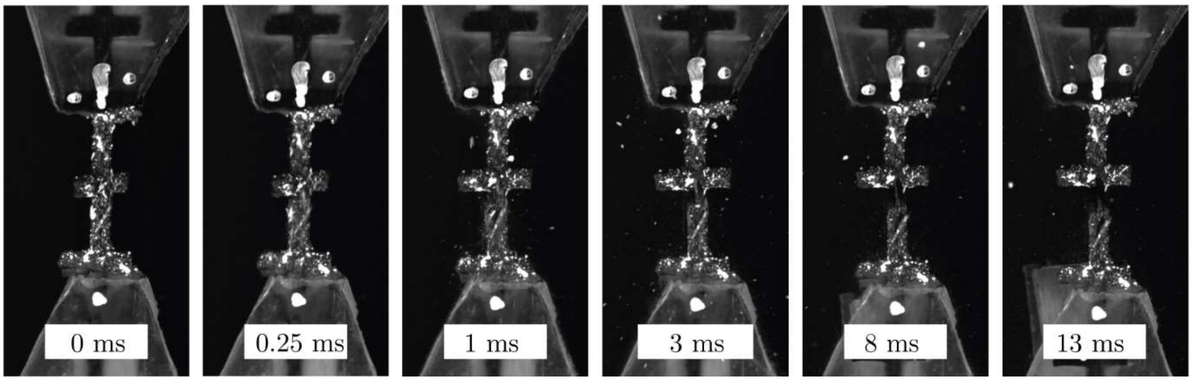

Figure 4. Rupture of the carbon-textile fabric

3. Tensile characterization of TRC integrating polyolefin fibres

An experimental programme was performed to characterize the tensile response of TRC, when the fabric is embedded in the micro-concrete. The aim was to investigate of the development of bond and potential failure modes.

3.1 Tensile specimens and test setup

The tensile specimens are ties measuring 800 mm in length, 100 mm in width, and with varying thicknesses of 20 mm, 30 mm or 40 mm. A total of 37 specimens were prepared, incorporating 0, 5 (V_f= 0.55 %)., or 10 kg/m³ (V_f = 1.1 %) of polyolefin fibres. The specimens were reinforced with a carbon-textile mesh placed in the middle of the cross-section, arranged either as a continuous layer or with overlaps of 40 mm, 80 mm, 120 mm, or 160 mm positioned at the mid-length of the specimen. The geometry of the specimens is presented in Figure 5 (a) and a detailed description of the specimen configurations is provided in [12].

Tensile tests were conducted using a conventional testing machine, with Digital Image Correlation (DIC) acquisition to track displacements and crack openings during the tests.

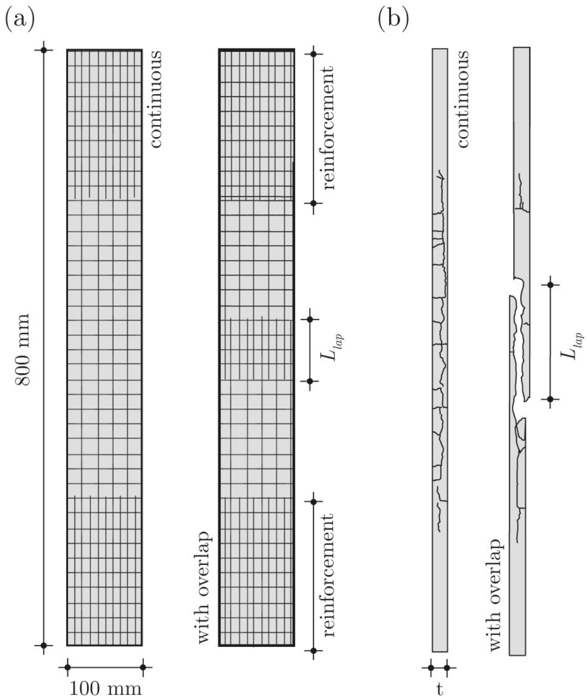

Figure 5. Tensile specimens: (a) geometry, (b) delamination phenomena

3.2 Tensile tests results

The results for selected 20 mm-thick specimens are presented and compared in Figure 6. Three specimens with a continuous mesh are analysed: specimen 20/0/C (0 kg/m³ of fibres), specimen 20/5T/C (5 kg/m³ of fibres), and specimen 20/10T/C (10 kg/m³ of fibres). The first two specimens exhibited the expected stress-strain response, with stiffness values closely matching the stiffness of a single roving. In contrast, the third specimen (20/10T/C) displayed a higher-than-expected strain, resulting in a shift of the stress-strain curve. Additionally, this specimen exhibited a longitudinal delamination crack (Figure 5 (b)), which was not observed in the other two specimens. For the three specimens, failure occurred suddenly, with a limited role of the fibres in the residual resistance and toughness after maximum load.

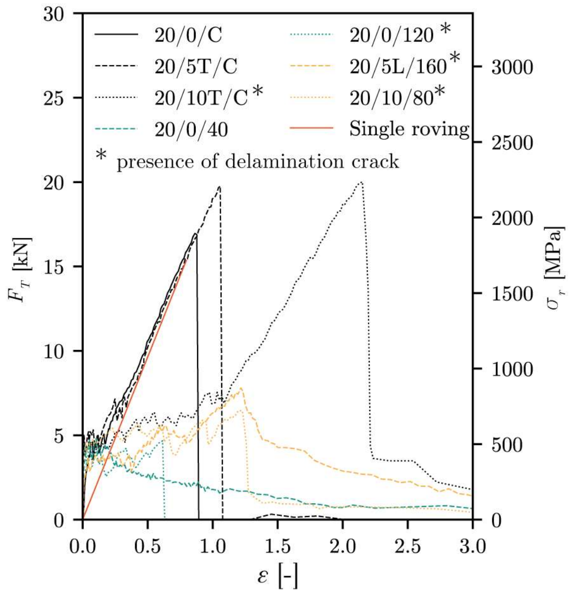

Figure 6. Tensile tests results for seven selected 20 mm-tick specimens

Four specimens with an overlapping length at the mid-section are also presented in the same figure, with the overlap intentionally designed as a weak zone governed by the pull-out of the fabric. Two specimens do not contain polyolefin fibres (0 kg/m³): Specimen 20/0/40 (40 mm overlap) and Specimen 20/0/120 (120 mm overlap). Additionally, one specimen includes 5 kg/m³ of fibres (Specimen 20/5/160 with a 160 mm overlap), and another incorporates 10 kg/m³ of fibres (Specimen 20/10/80 with an 80 mm overlap).

Specimen 20/0/40, with a 40 mm overlap, failed by pull-out of the fabric. The relatively short overlap length resulted in a low resistance, but the response had a significant toughness, which can be associated to the energy dissipated by friction between the textile fabric and the matrix during the pull-out process. The remaining three specimens developed on the contrary delamination cracks that led to the splitting of the specimen into two parts, as illustrated in Figure 5 (b). Notably, even with the addition of fibres, delamination cracks were not prevented. As shown in [12], specimens with an overlap length of 160 mm did not show delamination cracks. Instead, failure occurred by rupture of the fabric.

3.3 Delamination phenomena

As previously observed, some specimens have shown longitudinal delamination cracks as illustrated in Figure 5 (b). The development of these cracks is directly related to the orientation of the fabric within the specimen. All specimens showing delamination cracks have carbon-textile fabric oriented in the assumed 90º direction, while those without such cracks had fibres oriented perpendicularly, in the assumed 0º direction (according to the direction presented in Figure 1). The 0º orientation corresponds to a straight roving, whereas the 90º orientation results in undulated rovings as shown in Figure 7. This undulation generates deviation forces that can promote the formation of delamination cracks, as previously discussed in [15].

As the rovings are initially undulated, straightening can occur under tensile loading. In previous studies, straightening has been observed as a non-linear behaviour in single rovings subjected to tensile tests [7].

When embedded in concrete, the undulated rovings are bonded to the surrounding matrix, which restricts their movement and prevents complete straightening. This generates out-of-plane deviation forces, which may induce delamination cracks. Once a delamination crack originates, the filaments can straighten easily, which is reflected in an increase of length of the rovings. Such effect (increase of apparent strains in the tie) is thus consistent with the shift observed in the stress-strain curve observed in Specimen 20/10T/C (see Figure 6), as well as the reduced stiffness of the single roving. The additional strain is therefore directly linked to the geometrical properties of the rovings and the orientation of the applied load.

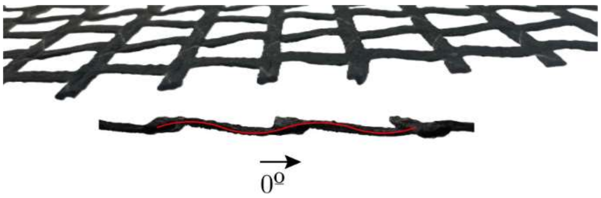

Figure 7. Undulated roving in the 0º orientation

3.4 Analytical model

Based on these observations, a simplified analytical model can be established, based on the Tension Chord Model [16]. For specimens with the carbon-textile oriented at 90º and showing a delamination crack, the model incorporates an additional strain to account for the straightening capacity of the rovings. This adjustment aligns with the mechanical behaviour observed in the experimental results.

The shape of the roving's undulation is approximated as a circular arc. Progressive straightening is assumed, with a smooth transition as a function of the applied stress level. Details on the model formulation and step-by-step implementation are provided in [12]. The comparison of the analytical model with the selected 20 mm-thick specimens is presented in Figure 8.

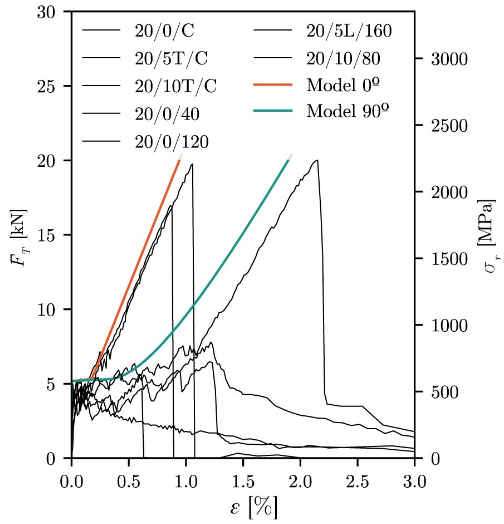

Figure 8. Comparison of experimental results with the analytical model.

4. Conclusions

This paper presents the results of experimental programs investigating the components of Textile Reinforced Concrete (TRC) and their combined behaviour as a composite material.

The main parameters for selecting an appropriate cementitious matrix and achieving optimal workability with polyolefin fibres have been identified. A self-compacting micro-concrete with a suitable water-to-cement ratio is essential to ensure uniform fibre distribution.

The characterization of the carbon-textile fabric is not straightforward, with the testing methodology and specimen typology playing a critical role in accurately determining the tensile strength. A specific specimen configuration was identified to prevent failure in the clamping zones or at the concrete interface, producing results consistent with the capstan grip testing method.

The bi-directional fabric considered shows two distinct orientations: straight rovings (assumed 0º) and undulated rovings (assumed 90º). When the straight rovings are aligned parallel to the applied load, the tensile behaviour of TRC resembles that of traditional reinforced concrete. However, when the undulated rovings are aligned parallel to the load, a delamination phenomenon occurs, leading to reduced apparent stiffness of the roving due to additional displacement from roving straightening. This phenomenon manifests as a shift in the TRC stress-strain relationship. The study also highlights the limited role of fibres in enhancing the post-peak tensile response of the composite material. Furthermore, the fibre content is constrained by the casting process for thin elements, and the amounts used were insufficient to prevent delamination.

A "fuse strategy," which involves incorporating weak overlapping regions to induce pull-out failure, remains a promising approach for improving material toughness. The resistance is however reduced and its effectiveness depends on mitigating delamination, with an overlap length for the tested parameters ranging between 40 mm and 160 mm.

A theoretical model, extending the Tension Chord Model to include the straightening of fabric rovings is outlined. This model predicts the tensile behaviour of TRC for cases with or without delamination.

Acknowledgements

This work has been performed within the frame of the research project PID2021-127920NB-I00 "A transition to sustainable construction using cementitious-based materials: Textile Reinforced Concrete for structural applications" funded by the call MCIN/AEI/10.13039/ 501100011033/FEDER,UE (Ministerio de Ciencia e Innovación, Agencia Estatal de Investigación, Spain, cofunded by the European Union). The authors would like to thank also the support by Holcim Spain for their technical assistance in the definition of the cementitious matrix, as well as S&P Spain (Iván Carracedo) for providing the fabrics for the test.

References

[1] U. N. Environment, K. L. Scrivener, V. M. John, and E. M. Gartner, "Eco-efficient cements: Potential economically viable solutions for a low-CO 2 cement-based materials industry ☆," 2018, doi: 10.1016/j.cemconres.2018.03.015.

[2] P. J. M. Monteiro, S. A. Miller, and A. Horvath, "Towards sustainable concrete," *Nat Mater*, vol. 16, no. 7, pp. 698–699, Jul. 2017, doi: 10.1038/nmat4930.

[3] A. Favier, C. De Wolf, K. Scrivener, and G. Habert, "A sustainable future for the European Cement and Concrete Industry - Technology assessment for full decarbonisation of the industry by 2050," Switzerland, 2018.

[4] G. Habert, "Assessing the environmental impact of conventional and 'green' cement production," in *Eco-efficient Construction and Building Materials*, Elsevier, 2014, pp. 199–238. doi: 10.1533/9780857097729.2.199.

[5] P. Valeri, P. Guaita, R. Baur, M. Fernández Ruiz, D. Fernández-Ordóñez, and A. Muttoni, "Textile reinforced concrete for sustainable structures: Future perspectives and application to a prototype pavilion," *Structural Concrete*, vol. 21, no. 6, pp. 2251–2267, Dec. 2020, doi: 10.1002/SUCO.201900511.

[6] C. H. Kulas, "Zum Tragverhalten getränkter textiler Bewehrungselemente für Betonbauteile".

[7] P. Valeri, M. Fernàndez Ruiz, and A. Muttoni, "Tensile response of textile reinforced concrete," *Constr Build Mater*, vol. 258, p. 119517, Oct. 2020, doi: 10.1016/J.CONBUILDMAT.2020.119517.

[8] M. G. Alberti, A. Enfedaque, D. M. V. Faria, and M. Fernández Ruiz, "The Potential of Fiber-Reinforced Concrete to Reduce the Environmental Impact of Concrete Construction," *Applied Sciences (Switzerland)*, vol. 14, no. 15, Aug. 2024, doi: 10.3390/app14156629.

[9] European Committee for Standadization (CEN), "EN 1015-3:1999: European Standard - Methods of test for mortar for masonry - Part 3: Determination of consistence of fresh mortar (by flow table)," 1999.

[10] European Committee for standardization (CEN), "EN-12390-3:2019: European Standard - Testing hardened concrete - Part 3: Compressive strength of test specimens," 2019.

[11] European Committee for Standardization, "EN 12390-5:2019 : European Standard - Testing hardened

concrete - Part 5: Flexural strength of test specimens," 2019.
[12] J. Devènes *et al.*, "Tensile response of Textile Reinforced Concrete incorporating synthetic fibres," *Under-reviewed / Construction and Building Materials*, 2025.
[13] S&P, "ARMO-mesh ® Reinforcement mesh made from carbon fibre," Nov. 2023. [Online]. Available: www.sp-reinforcement.eu
[14] Sika, "Sikadur®-52 Injection LP," Mar. 2023. Accessed: Dec. 17, 2024. [Online]. Available: file:///C:/Users/Julie/Downloads/sikadur-52-injectionlp.pdf
[15] P. Preinstorfer, S. Yanik, J. Kirnbauer, J. M. Lees, and A. Robisson, "Cracking behaviour of textile-reinforced concrete with varying concrete cover and textile surface finish," *Compos Struct*, vol. 312, p. 116859, May 2023, doi: 10.1016/j.compstruct.2023.116859.
[16] P. Marti, M. Alvarez, W. Kaufmann, and V. Sigrist, "Tension Chord Model for Structural Concrete," *Structural Engineering International*, vol. 8, no. 4, pp. 287–298, Nov. 1998, doi: 10.2749/101686698780488875.